Chemical parameters influencing fine-tuning in the binding of macrolide antibiotics to the ribosomal tunnel

Erez Pyetan, David Baram, Tamar Auerbach-Nevo,
and Ada Yonath

Department of Structural Biology, the Weizmann Institute of Science,
76100 Rehovot, Israel

Pure Appl. Chem., Vol. 79, No. 6, pp. 955–968, 2007.
doi:10.1351/pac200779060955

Chemical parameters influencing fine-tuning in the binding of macrolide antibiotics to the ribosomal tunnel*

Erez Pyetan†, David Baram†, Tamar Auerbach-Nevo, and Ada Yonath‡

Department of Structural Biology, the Weizmann Institute of Science, 76100 Rehovot, Israel

Abstract: In comparison to existing structural, biochemical, and therapeutical data, the crystal structures of large ribosomal subunit from the eubacterial pathogen model *Deinococcus radiodurans* in complex with the 14-membered macrolides erythromycylamine, RU69874, and the 16-membered macrolide josamycin, highlighted the similarities and differences in macrolides binding to the ribosomal tunnel. The three compounds occupy the macrolide binding pocket with their desosamine or mycaminose aminosugar, the C4-C7 edge of the macrolactone ring and the cladinose sugar sharing similar positions and orientations, although the latter, known to be unnecessary for antibiotic activity, displays fewer contacts. The macrolactone ring displays altogether few contacts with the ribosome and can, therefore, tilt in order to optimize its interaction with the 23S rRNA. In addition to their contacts with nucleotides of domain V of the 23S RNA, erythromycylamine and RU69874 interact with domain II nucleotide U790, and RU69874 also reaches van der Waals distance from A752, in a fashion similar to that observed for the ketolides telithromycin and cethromycin. The variability in the sequences and consequently the diversity of the conformations of macrolide binding pockets in various bacterial species can explain the drug's altered level of effectiveness on different organisms and is thus an important factor in structure-based drug design.

Keywords: ribosomes; macrolides; erythromycylamine; RU69874; josamycin.

INTRODUCTION

Abbreviations

E50S	large ribosomal subunit from *E. coli*
D50S	large ribosomal subunit from *Deinococcus radiodurans*
H50S	large ribosomal subunit from *Haloarcula marismortui*
mH50S	large ribosomal subunit from *Haloarcula marismortui* in which a G→A mutation was carried out in position 2099Hm (2058Ec) of the 23S rRNA.

Ribosomes are giant ribonucleoprotein cellular assemblies, translating the genetic code into proteins. They are built of two subunits of unequal size, which in eubacteria are of molecular weights of 0.85 and

*Paper based on a presentation at the 18th International Conference on Physical Organic Chemistry (ICPOC-18), 20–25 August 2006, Warsaw, Poland. Other presentations are published in this issue, pp. 955–1151.

†These authors contributed equally to this work.

‡Corresponding author: E-mail: ada.yonath@weizmann.ac.il

1.45 MDa. The small subunit (called 30S in prokaryotes) contains about 20 proteins and an RNA chain, called 16S, of about 1500 nucleotides. The large subunit (called 50S in prokaryotes) contains 31–35 proteins and about 3000 nucleotides, arranged in two RNA chains. The short chain is called 5S RNA, and the very long one, composed of 5 structural domains, is called 23S RNA. The two ribosomal subunits assemble upon the initiation of the process of protein biosynthesis to form the functionally active ribosome (called 70S in prokaryotes). While elongating, the small subunit provides the decoding center and controls translation fidelity, whereas the large subunit catalyzes peptide bond formation at its peptidyl transferase center (PTC), and provides the exit tunnel along which the newly born proteins progress until they emerge out of the ribosome. Messenger RNA (mRNA) carries the genetic code to the ribosome, and the amino acids are brought to the ribosome by their cognate transfer RNA (tRNA) molecules, built as L-shaped double helices with their two functional sites, the anticodon loop and the aminoacylated 3' end, located at their opposite edges as single strands. The ribosome possesses three tRNA binding sites, the A-(aminoacyl), the P-(peptidyl), and the E-(exit) sites, each of which resides on both subunits. The tRNA anticodon loops interact with the mRNA on the small subunit, whereas the aminoacylated or peptidylated tRNA 3' ends are positioned in the large subunit. Each elongation cycle involves decoding, creation of a peptide bond, and release of a free tRNA molecule. It requires the advancement of the mRNA together with three tRNA molecules from the A- to the P- and then to the E-sites, a motion driven by GTPase activity.

Being a central element of the cell's life cycle, the ribosome is a main target for a broad range of antibiotics [1–7], and although ribosomes are highly conserved they possess subtle, albeit critical, sequence and/or conformational variations, which facilitate drug selectivity, thus enabling clinical usage. Comprehensive biochemical and crystallographic studies showed that the ribosomal antibiotics target distinct locations within ribosomal functional sites and exert their inhibitory action by diverse modes, such as competing with substrate binding, interfering with ribosomal dynamics, minimizing or eliminating ribosomal mobility, causing miscoding, hampering the motions of the mRNA chain, and preventing the progression of the nascent proteins by blocking the exit tunnel. Detailed analysis of the similarities and variability in antibiotics' binding site has been and still is the subject of intensive biochemical and crystallographic studies aimed at improving drug selectivity while minimizing drug resistance.

Very few ribosomes, none of which are genuine pathogens, have been crystallized, so crystallographic analysis of antibiotics binding to ribosomes is hitherto limited to those species that mimic pathogens. The large ribosomal subunit from the eubacterium *Deinococcus radiodurans* (D50S), for which the high-resolution crystal structure had been determined [8], provides an excellent model since it is inhibited by ribosomal antibiotics in a fashion similar to pathogens, binds many of the antibiotics targeting ribosomes at clinically relevant concentrations, and since these therapeutical meaningful complexes yielded well-diffracting crystals. Common traits detected in the structures of over a dozen of these complexes [9–15] revealed that ribosomal antibiotics interact mostly with the ribosomal RNA, and although theoretically the ribosome offers many different binding sites for these small compounds, multiple sites are scarce [3,4].

Macrolides, which account for over 40 % of the clinically useful antibiotics, inhibit protein biosynthesis in bacteria by blocking the ribosomal tunnel at a specific site, composed of nucleotides of domain V of the 23S rRNA. This site is located in proximity to the PTC, allowing short peptides of about 5–7 residues to be formed before reaching it. Macrolides consist of a 12–18-membered macrolactone ring with various substituents, as well as 1–3 neutral and/or amino sugars (Fig. 1). The first macrolide in clinical use against gram-positive bacteria was the naturally occurring 14-membered ring erythromycin [1,2,16]. However, its acid instability, poor bioavailability, and unpredictable pharmacokinetics led to the development of the second-generation macrolides, which are semisynthetic derivatives of erythromycin. Indeed, many of these advanced macrolides display excellent pharmacokinetics, bind to ribosomes with a higher affinity, and are generally more active against rRNA mutants than their parent drug [16–21]. For instance, methylation of the hydroxyl group at C6 (Fig. 1) produced the po-

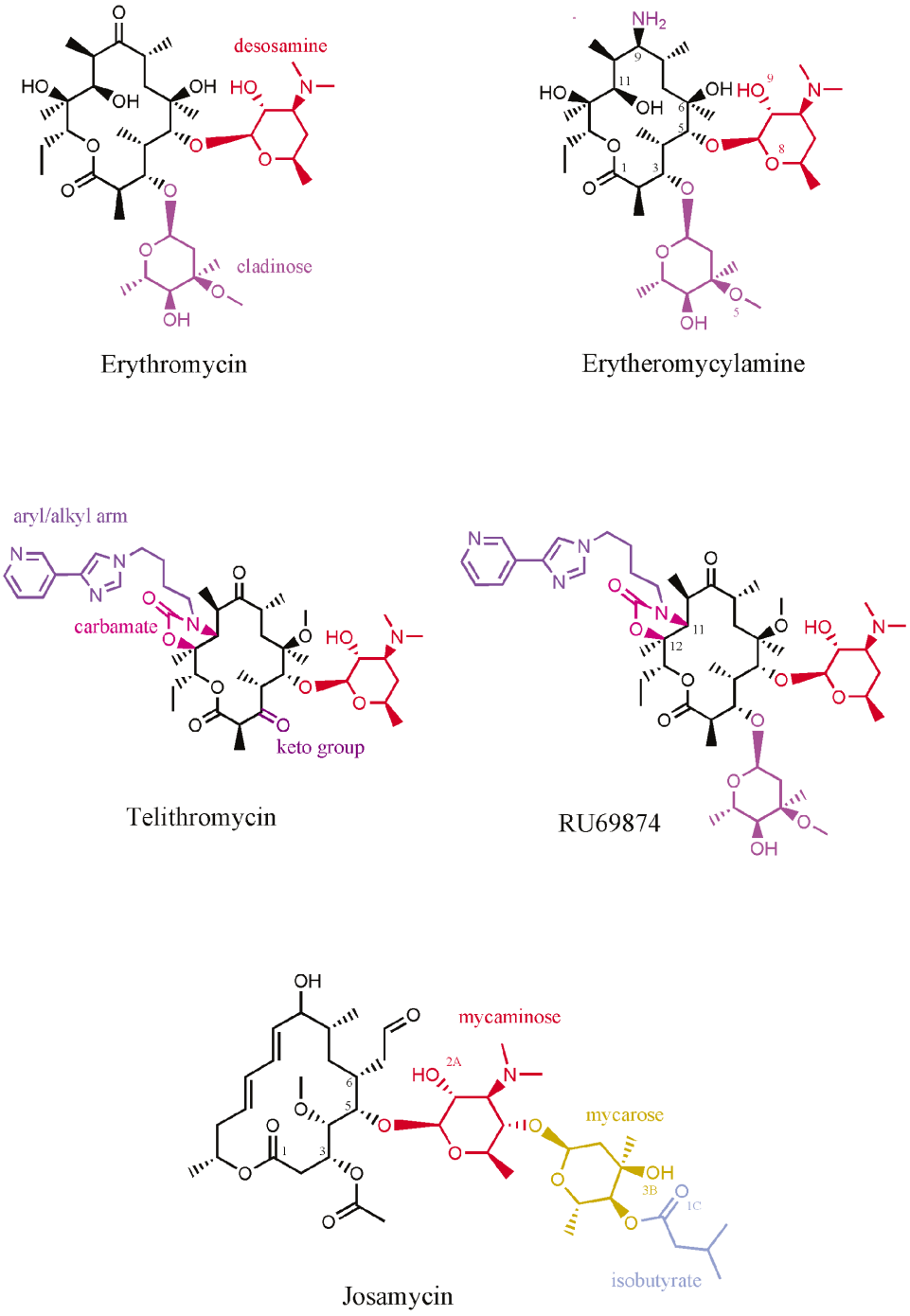

Fig. 1 Chemical structures of erythromycin, erythromycylamine, telithromycin, RU69874, and josamycin.

tent and acid-stable drug clarithromycin, while increasing the drug's flexibility by the addition of a single nitrogen to the macrolactone ring at position 9 (Fig. 1) yielded the 15-membered ring azithromycin, which displays also improved microbiological activity against gram-negative bacteria [16].

An additional reason for the development of advanced macrolides is the spread of resistance to macrolide antibiotics (Fig. 1), a major problem in modern therapeutics. A common resistance mechanism is increasing the bulkiness of moieties that play central roles in antibiotic binding, hence imposing spatial constrains and hampering macrolide binding. Within this frame, the naturally occurring macrolides have undergone chemical manipulations that produced a large collection of antimicrobial macrolide agents. Most of these compounds are based on the addition of chemical moieties to existing drugs, which can reach new anchoring sites on the ribosome, thus compensating for the loss of the interactions caused by the increased bulkiness of the critical binding moiety. Among these are the ketolides, in which the typical 14-membered macrolactone ring and the desosamine sugar at position C5 are retained, whereas the cladinose sugar at position C3 is substituted by a keto group, an 11,12 cyclic carbamate replaces two hydroxyl groups, and an aryl/alkyl or a quinolylallyl chain is linked to the molecule. Telithromycin (Fig. 1), the first ketolide approved for clinical use, displays excellent pharmacokinetics, binds to the ribosome with higher affinity, and is generally more active against rRNA mutants than its parent drug.

Numerous biochemical and genetic studies have indicated that the identity of the nucleotide at position 2058 of the 23S RNA is critical for 14-membered ring macrolide binding. Thus, adenosine (A) in this position, as in most eubacterial ribosomes, permits binding, whereas species with guanosine (G) at 2058, namely, eukaryotes and most archaea, do not bind macrolides. Consistently, bacterial strains resistant to 14-membered macrolides commonly contain the mutation A→G at position 2058 or a methylation of its exocyclic N6 amine by methyltransferase enzymes [22–25]. The crystal structures of D50S with several 14-membered macrolides (erythromycin, clarithromycin, roxithromycin, and troleandomycin), a 15-membered macrolide (azithromycin), and ketolides (telithromycin and cethromycin, also called ABT-773) provided first-hand insight into macrolide and ketolide modes of action and confirmed the involvement of nucleotide 2058 in the drugs' interactions with the ribosome [9–13].

Consistently, the large ribosomal subunit of the archaeon *Haloarcula marismortui* (H50S), which carries G at the position corresponding to 2058 of the 23S rRNA, does not bind 14-membered macrolides [26] and required extremely high drug concentrations for binding the 15- and 16-membered ring macrolides [27]. However, G→A mutation at position 2058, which yielded an archaeon ribosome that resembles eubacteria in this respect (here called mH50S), increased substantially its affinity to several macrolides and ketolides and allowed the determination of the crystal structure of its complex with the 14-membered macrolide erythromycin and the ketolide telithromycin [26]. Comparisons between the binding modes observed in eubacteria to that detected in the mutated archaeal ribosome indicated that although bound approximately to the same region of the large ribosomal subunit, the various substituents of the macrolides on one hand, and the species diversity on the other, result in substantial differences in the exact binding modes [28,29], implying that mere binding does not assure effective inhibitory action. Hence, this comparison illuminated subtle, albeit crucial, details in macrolide binding modes, thus it shed light on the parameters governing significant variability in activity and potency among bacterial species and highlighted key factors contributing to diversity in antibiotics action.

For performing more extensive analysis, we determined the structures of complexes of D50S with three macrolide antibiotics: erythromycylamine [30], RU69874 [31], and josamycin [32]. Erythromycylamine is a second-generation macrolide, obtained by nonenzymatic hydrolysis during intestinal absorption of dirithromycin, a semisynthetic macrolide antibiotic designed for oral administration. The result of this hydrolysis, erythromycylamine, is almost identical to erythromycin, but the typical keto group at position C9 of the macrolactone ring is replaced by an amine (Fig. 2). RU69874 is a typical 14-membered ring macrolide that carries two sugar moieties, but its –OH groups at positions 11, 12 are replaced by a cyclic carbamate, which carries an aryl/alkyl (Fig. 1) in a fashion identical to that of the potent ketolide telithromycin. Josamycin, a potent macrolide antibiotic from *Streptomyces narbonensis*, belongs to the subgroup of natural 16-membered macrolides, which have a disaccharide extension at position C5 of the macrolactone ring, as opposed to the monosaccharide desosamine present in the

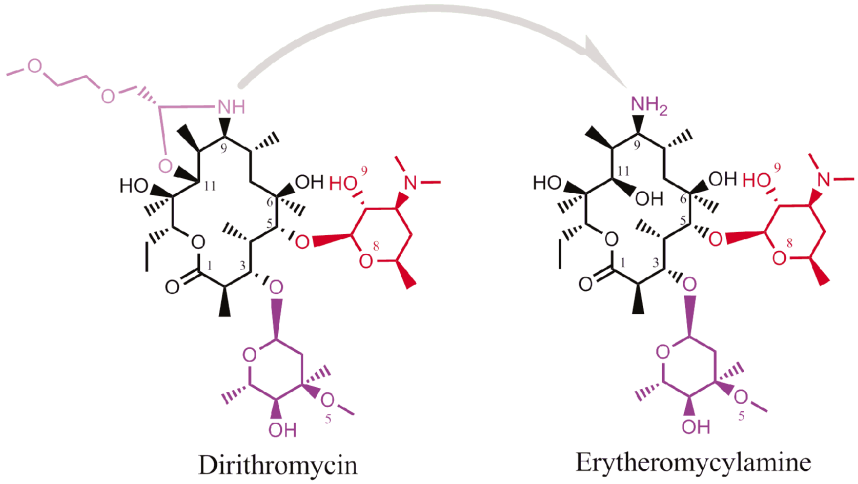

Fig. 2 Dirithromycin (left) and the result of its hydrolysis, erythromycylamine (right).

14- and 15-membered macrolides [16]. It carries an ethyl-aldehyde group at position C6 of the lactone ring and a mycaminosyl–mycarosyl–isobutyrate moiety at C5 (Fig. 1).

Here we present the structures of these three macrolides within a frame of a comprehensive analysis of the binding modes of all known macrolides and ketolides. This study elucidated the relative significance of each of the interactions of the ribosome with the various substituents of the macrolactone ring and highlighted the nucleotides of the 23S rRNA involved in the drugs' binding. It also highlighted the discrepancies between macrolide complexes with representatives of eubacteria, archaea, and a mutated species sharing properties with both eubacteria and eukaryotes. The considerable variability in the details of antibiotic binding and inhibitory modes observed by this comparison justifies expectations for structure-based improved antibiotics properties.

RESULTS

Erythromycylamine: A potent 14-membered macrolide

The 3.6 Å crystal structure of erythromycylamine complexed with D50S reveals (Figs. 3A, D) that erythromycylamine is located within the large ribosomal subunit in the common macrolide binding pocket and interacts mainly with nucleotides of domain V of the 23S rRNA. Its desosamine and cladinose sugars attain similar positions to those of erythromycin in complex with D50S [9,33] and mH50S [26]. Consistent with previous biochemical and structural data, the O8 of the desosamine sugar forms a hydrogen bond with the highly conserved nucleotide A2058. Other hydrogen bonds are observed between nucleotide A2062 and O9 of the desosamine sugar, and between nucleotide G2505 and the etheric O5 of the cladinose sugar. Notably, all three nucleotides A2058, A2062, and G2505 have been previously indicated as particularly important for the binding of MLS_B (macrolide, lincosamide, and streptogramin B) antibiotics to eubacterial ribosomes. Other nucleotides of domain V involved in hydrophobic interactions with the drug are A2059, U2609, C2610, and C2611. An additional interaction, not observed for erythromycin, is a hydrogen bond between nucleotide U790 of domain II of the 23S RNA and the unique amino group on C9 of erythromycylamine. This interaction can account for the slight tilt in the orientation of the macrolactone ring with respect to erythromycin in all the known crystal forms of its complex with the large ribosomal subunit [9,26,33].

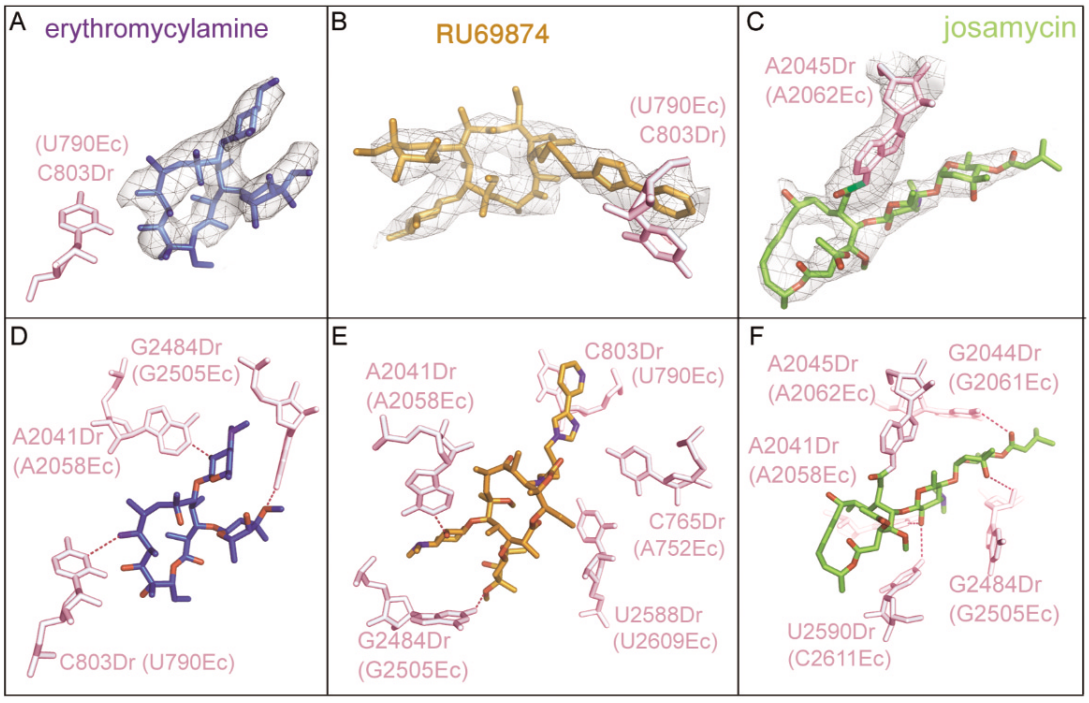

Fig. 3 Macrolide interactions with their binding sites. (A–C) the unbiased 2Fo-Fc electron-density maps for (A) erythromycylamine, (B) RU69874, and (C) josamycin, in D50S (contoured at 1.5σ). Note the continuous electron density for the covalent bond between josamycin and nucleotide A2045Dr (A2062Ec). (D–F) interactions between the macrolides (D) erythromycylamine (blue), (E) RU69874 (orange), and (F) josamycin (green) and D50S nucleotides, of which only those located closest to the bound drug are shown (in gray–purple). Note RU69874 binding to domains V and II, with its aryl/alkyl arm stacking to C803Dr (U790Ec) and the shortest distance to nucleotide C765Dr (A752Ec) being 3.4 Å. Nucleotide U2588Dr (U2609Ec) is shown for comparison, as it was reported to interact with telithromycin in mH50S [26].

RU69874: A macrolide with ketolide properties

The 3.6 Å crystal structure of RU69874 in complex with D50S (Figs. 3B, E) reveals that the conformation and the position of the lactone ring of RU69874 are similar to those observed for erythromycin and telithromycin bound to D50S [13,33] and to mH50S [26], but its orientation is slightly tilted compared to that of erythromycylamine (Fig. 4A). Despite the differences between RU69874 and erythromycylamine chemistry, both interact well with the tunnel walls. 1419.7 $Å^2$ (57 %) of RU69874 surface area is buried in its complex with D50S, compared with 1220.86 $Å^2$ (63 %) of erythromycylamine surface area. Furthermore, the positions and orientations of the sugar moieties are similar to those of erythromycylamine; in particular, the desosamine sugar aligns perfectly (Fig. 4B). Consistently, the interactions of these moieties with nucleotides of domain V of the 23S rRNA are similar to those detected in the complex of D50S with erythromycylamine. Interestingly, in addition to its interactions with domain V nucleotides, RU69874 reaches also nucleotides of domain II of the 23S rRNA, which is positioned across the tunnel. Thus, its aryl/alkyl extension attains an overall conformation similar to that observed for the telithromycin-D50S complex, and consistently stacks to nucleotide U790 of domain II of the 23S rRNA [13,33]. This arm lies in close proximity to domain II nucleotide A752 (the shortest distance between the nucleotide N4 and the aryl/alkyl arm being 3.4 Å), a nucleotide that was found biochemically to be effected by telithromycin binding [7,34].

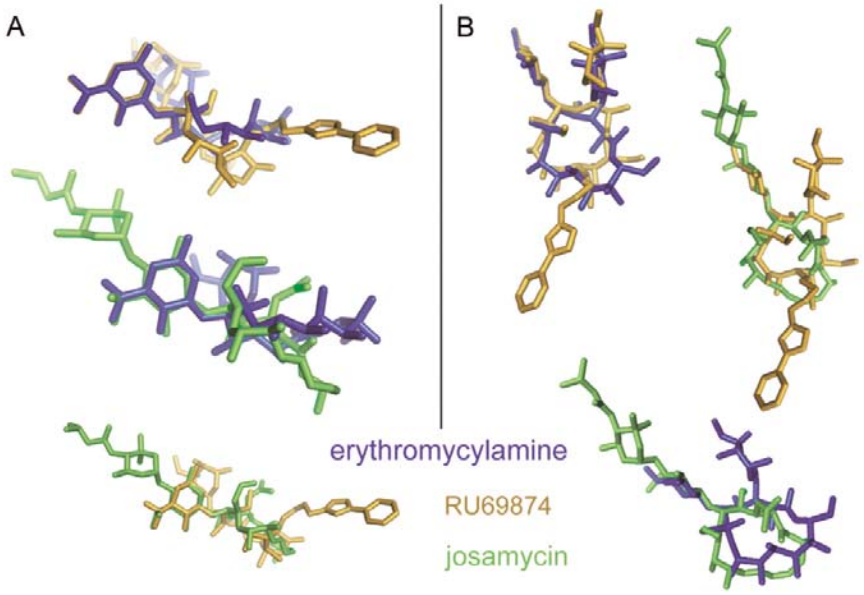

Fig. 4 Similarities and variability in macrolide binding modes to the ribosome. Superimpositions of the macrolides bound to D50S. (A) Side view (B) Face view.

Josamycin: A 16-membered macrolide

Crystals of D50S soaked in solutions containing josamycin diffracted up to 3.0 Å, yielding a 3.3 Å (Table 1) structure. The electron-density map of this complex was sufficiently detailed for accurate determination of the drug's conformation and binding site (Fig. 3C). It is noteworthy that, similar to RU69874 and erythromycylamine, 60 % (1383.77 $Å^2$) of josamycin surface area is buried in its complex with D50S. Although josamycin binds in the ribosomal tunnel, it only partially overlaps the 14-membered macrolide binding site. Notably, the majority of its contacts involve the ethyl-aldehyde group at position C6 and the mycaminosyl–mycarosyl–isobutyrate moiety at position C5 (Fig. 3F). The strongest interaction between josamycin and the 23S rRNA is a covalent bond formed between the aldehyde substitute at the C6 of the 16-membered lactone ring and the exocyclic N6 amino group of A2062, similar to the interaction reported for the complex of carbomycin A with H50S [27]. The mycaminosyl–mycarosyl–isobutyrate moiety at position C5 of josamycin's lactone ring forms several hydrogen bonds in the tunnel proximate to the PTC, in addition to an extensive network of hydrophobic contacts. The mycaminose sugar aligns almost perfectly with the desosamine sugar of the 14-membered macrolides (Fig. 4B), and consistently, its oxygen 2A forms a hydrogen bond with N1 of A2058. This oxygen also offers possible hydrogen bonding to C2611, and oxygen 3B of the mycarose sugar appears to form a hydrogen bond with G2505 and the carbonyl oxygen 1C of the isobutyrate shares a hydrogen bond with G2061. The nucleotides located between the tunnel and the PTC, namely, G2061, A2451, U2506, and U2585, are highly conserved. Consistently, the position and orientation of the mycarose and isobutyrate moieties, which interact with these nucleotides, are almost identical in both carbomycin-H50S [27] and josamycin-D50S complexes.

Table 1 Crystallographic statistics. (Numbers in parentheses denote the highest-resolution bin.)

	Erythromycylamine	RU69874	Josamycin
Space group	I222	I222	I222
Unit cell parameters (Å)	*a* = 170.437, *b* = 413.538, *c* = 693.720	*a* = 170.010, *b* = 412.423, *c* = 695.379	*a* = 172.802, *b* = 411.475, *c* = 697.616
Resolution range (Å)	20–3.6 (3.73–3.6)	30–3.6 (3.73–3.6)	20–3.3 (3.42–3.3)
# of unique reflections	251 286	226 136	345 218
Completeness (%)	89.8 (79.0)	83.9 (75.0)	95.5 (89.3)
Redundancy	6.5 (5.0)	2.2 (1.9)	3.2 (2.3)
R_{sym} (%)	20.6 (47.1)	17.7 (53.7)	18.4 (48.0)
$\langle I \rangle / \langle \sigma(I) \rangle$	4.9 (1.6)	4.2 (2.0)	4 (1.5)
R (%)	28.07	28.30	28.2
R_{free} (%)	34.13	36.44	33.05
Bond distance r.m.s (Å)	0.008	0.008	0.0087
Bond angle r.m.s	1.4°	1.47°	1.45°

DISCUSSION

Linking location, binding duration, specific interactions, and potential drug effectiveness

Although all macrolides bind to the same region of the ribosomal tunnel, the exact locations of their different substituents vary. Thus, most 14-membered macrolides, including the newly determined erythromycylamine and RU69874, allow passage of the first 5–7 amino acids of the nascent polypeptide in the ribosomal tunnel. In comparison, similar to carbomycin A [27], josamycin's disaccharide substituent at position C5 extends toward the PTC (Fig. 5A) and therefore can interfere with formation of the first or second peptide bond. This location accords with the finding that contrary to 14-membered macrolides, 16-membered macrolides with a disaccharide substituent at position C5 inhibit the peptidyltransferase reaction itself [35]. Indeed, kinetic and biochemical studies have shown that josamycin slows down the formation of the first peptide bond and, depending on peptide sequence, may completely inhibit formation of the second or third peptide bond [36].

Josamycin's covalent bond with the 23S RNA may explain its long lifetime on the ribosome (3 h), in comparison with erythromycin (less than 2 min) [36]. It may also explain the increase in MIC values when the aldehyde group of 16-membered macrolides is reduced to an alcohol [37]. Consistently, nucleotide A2062 was shown to be strongly protected by carbomycin and tylosin binding in DMS probing experiments [35], and its mutations to G, C, and U conferred resistance to josamycin in *Streptococcus pneumoniae* [38], *Mycoplasma pneumoniae* [39], and *Mycoplasma hominis* [40].

Diversity and conservation in binding conformations

Analysis of the known structures of the macrolides' complexes revealed common patterns for each of their main structural elements: the macrolactone ring, the desosamine/mycaminose aminosugar, and the cladinose sugar. This analysis also identified a linkage between their binding traits and their chemical nature. Not surprisingly, the macrolides' auxiliary structural elements, namely, moieties obtained by chemical modifications, form chemical-driven interactions with ribosome nucleotides. In particular, most of the added long extensions expand across the tunnel and reach its opposite side.

The sugars: Among the common features displayed by the three new macrolides when bound to the ribosomal tunnel of D50S, are the positions and orientations of the desosamine sugar (mycaminose in the josamycin case), which are almost identical for the three of them (Fig. 4B). This observation is

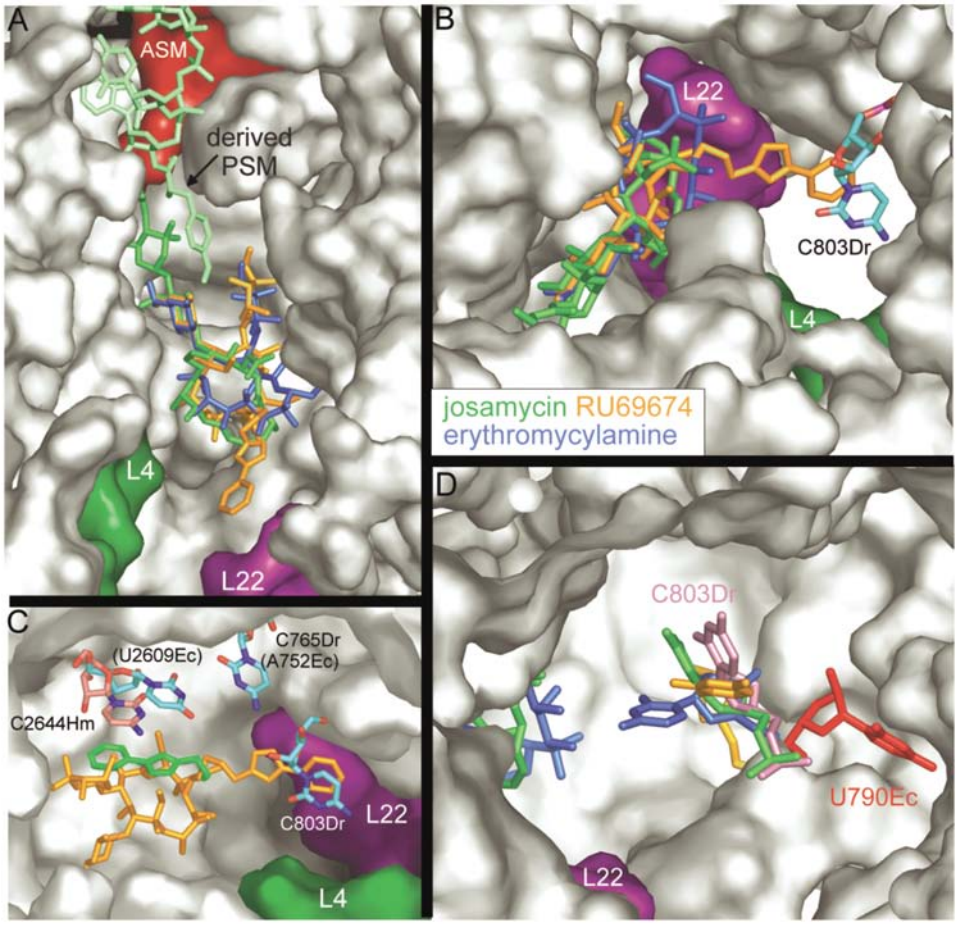

Fig. 5 Macrolide binding in the ribosomal tunnel. In all, ribosomal regions in proximity of the tunnel are shown as gray surface. (A) Transverse section of the upper part of the ribosomal tunnel, proximate to the PTC. The three macrolides, erythromycylamine (blue), RU69874 (orange), and josamycin (green), bind above the L4/L22 constriction (surface representation of L4 is in forest green and of L22 in purple). The isobutyrate moiety of josamycin reaches the PTC and overlaps the A-site (based on the structure of D50S complex with a 35- nucleotide chain mimicking the acceptor stem and the 3' terminus (called ASM and shown in ruby red) [53; PDB 1NJP]. For better orientation, the symmetry-derived P-site tRNA mimic, PSM, is shown in pale green. (B) View of the ribosomal tunnel from the PTC. Note the kink at the tunnel L4/L22 constriction (which is seen on the right), the macrolide binding pocket (occupying its narrow part, seen to the left), and its wider region. Slightly above L4/L22 constriction, C803Dr (in cyan), the counterpart of U790 in *E. coli* (sequence-wise, but not in orientation), is located at the opposite side, and points into the tunnel interior. (C) In D50S, RU69874 aryl/alkyl arm stretches all the way to the L4/L22 constriction, and stacks to C803Dr (U790Ec), as opposed to its position in mH50S (shown by itself in bright green), where it stacks to C2644Hm (corresponding to U2609Ec, seen in salmon pink) [26; PDB 1YIJ]. Note that this nucleotide occupies a different position and displays a different orientation from those observed for the corresponding *D. radiodurans* and *E. coli* nucleotides U2609Ec, U2588Dr [53; PDB 1NJP] and [47; PDB 2AW4]. (D) View of C803Dr from the position of protein L4 in the wide part of the tunnel, below the L4/L22 constriction. Four conformations of C803Dr and its counterparts are shown, as observed in the complexes of the three macrolides (colors correspond to those of the macrolides) as well as the native structure (gray). Nucleotide U790Ec in *E. coli* [47, PDB 2AW4] is shown in red. The tips of the lactone rings of josamycin and erythromycylamine are shown on the left.

consistent with previously published structures of D50S in complex with other members of the macrolide-ketolide family [9,11,13,33], as well as with the complexes of macrolides with H50S [27] and mH50S [26]. The conserved placement of the desosamine sugar and its importance to the drug's effective binding are further manifested by the fact that chemical manipulations on this sugar, as in the troleandomycin case [12], result in a significant alteration of the drug's binding conformation. The cladinose sugar forms fewer contacts in the tunnel than the desosamine and is not critical for binding, as indicated by its absence in ketolides and 16-membered macrolides. Nevertheless, it attains a similar position in the different structures, although less pronounced compared to that of the desosamine sugar. Consistently, the conserved nucleotide G2505, which interacts with it, displays slight shifts among the different structures, while the conformations of nucleotides A2058 and A2059, interacting with the desosamine sugar, remain unchanged.

The macrolactone ring: The interactions of the macrolactone ring of different macrolides with the 23S rRNA can vary significantly (e.g., Fig. 4A), since apart from a hydrogen bond in the erythromycylamine case, all its other contacts with the ribosome are less specific hydrophobic interactions. In general, the placement and orientation of the macrolactone ring appears to be determined by the unique position of the desosamine sugar and by the hydrophobic interactions of its C4-C7 edge. Yet, the macrolactone ring appears to acquire the conformation that seems to maximize the interactions of its substituents with nucleotides in the vicinity of the binding pocket, thus highlighting the freedom of the drug's scaffold to adapt a conformation most suited to accommodate the largest number of contacts in the tunnel.

The aryl/alkyl extension: In RU69874 complex with D50S, the aryl/alkyl extension attains an overall conformation similar to that observed for the telithromycin-D50S complex and consistently stacks to nucleotide U790 of domain II of the 23S rRNA [13,33]. Furthermore, in accord with the reported loss of the A752 footprint in *E. coli* ribosome upon telithromycin binding [7,34], the aryl/alkyl extension lies in a distance permitting van der Waals interactions. The cross-tunnel interactions of RU69874 aryl/alkyl extension explain why in some respects, such as its MIC values, it is similar to telithromycin [31] or even superior to it in several species. For example, in the gram-positive bacteria *Mycobacterium tuberculosis*, RU69874 MIC values are lower by 337-fold in comparison with telithromycin [20]. Nevertheless, previous studies have indicated that unlike telithromycin, RU69874 is a strong inducer of MLS_B resistance in several bacterial strains, including gram-positive *Streptococcus aureus*, *Streptococcus pyogenes*, and *S. pneuoniae.* Analysis of the contributions of the various substituents of RU69874 to its binding mode indicates that this unfavorable property originates from the existence of the cladinose sugar, which is eliminated in telithromycin and most ketolides. Interestingly, in D50S, the orientation of the aryl/alkyl arm of RU69874 is similar to that of telithromycin, regardless of the existence of a cladinose sugar, consistent with biochemical and genetics observations. This indicates that when stretched, the aryl/alkyl arm can form strong interactions with domain II components across the tunnel. When folded, however, this arm interacts solely with domain V, as observed in the crystal structure of mH50S telithromycin complex [26], and confirmed biochemically (A. Mankin, private communication).

To conclude: as noted earlier [3,4,33,42], the known structures of macrolide complexes with large ribosomal subunits reveal that the orientation of the side chains may substantially differ, but the overall position and conformation of the lactone ring is rather similar. The diversity in binding modes of macrolides possessing chemical differences accords well with the finding that subtle alterations in the macrolide binding pocket, such as a replacement of a canonic base pair (2057–2611) from A-U to G-C, influences telithromycin susceptibility and fitness cost in macrolide resistance mutants [41,42]. The comparison between the various binding modes observed in complexes of the 15-membered macrolide azithromycin to D50S, H50S, and mH50S shed more light on the interplay between the mode of the macrolide binding and the chemical nature of the various binding pocket constituents. Remarkably, in the case of azithromycin, the impressive gain in drug affinity achieved by the G2058A mutation is not accompanied by a comparable alteration in the orientation of the azithromycin within the binding

pocket [26], compared to H50S wild-type where 2058 is a guanosine. This seemingly surprising finding indicates that although 2058 identity determines binding affinity, the conformations and chemical identities of the other nucleotide in the macrolide pocket govern the antibiotic binding modes.

Effects of macrolide binding on the 23S rRNA

The 23S nucleotides of *D. radiodurans* that are critical for macrolide binding can be divided into two main groups. In one, containing A2058, A2059, G2061, C2610, and C2611, the positions and orientations of the nucleotides are not affected significantly by their interactions with the various macrolides, whereas the members of the second group, namely, nucleotides G2505, A2062, and U790, undergo conformational alterations, in a fashion depending on the chemical nature of the bound macrolide. For example, the conformation of nucleotide G2505 in the josamycin complex is similar to that observed in the native structure. However, in the complexes of erythromycylamine or RU69874 the orientation of this base is shifted to form a hydrogen bond with the cladinose sugar. Nucleotide A2062 also displays slight conformational alterations from its native structure in several macrolide complexes, including the three new compounds described here. In the erythromycylamine and RU69874 cases, the base's plane is tilted to allow for a hydrogen bond with the desosamine sugar, whereas in the josamycin complex, this base is slightly shifted to accommodate the covalent bond of the ethyl-aldehyde substituent of the lactone ring.

U790 of domain II is an example for a marked alteration of the binding pocket conformation induced by drug binding. Situated in a strategic position above the tunnel constriction (called L4/L22 constriction since proteins L4 and L22 are constituents of the tunnel wall at that location), and pointing into its interior, nucleotide U790 of the 23S rRNA seems to have a substantial effect on the conformation of telithromycin, RU69874 and erythromycylamine, hence it is likely to influence the overall strength of the macrolide–ribosome interactions. In D50S, this nucleotide undergoes considerable rearrangements upon macrolide binding (Fig. 5D). Thus, erythromycylamine causes its tilt by approximately 90°, compared to its native structure, resulting in the formation of a hydrogen bond with the amine group on C9 of the lactone ring. The inherent flexibility of this nucleotide is also exploited for binding RU69874. Thus, in this complex it is tilted by approximately 60° in a different direction, to allow stacking with the aryl/alkyl arm, similar to that observed for telithromycin when bound to D50S [13,33].

Cross-tunnel binding: Macrolides interacting with domain II

A752 of domain II, which resides on the tunnel wall across the macrolide binding pocket, was proposed to be directly involved in macrolides binding since it was found to footprint in *E. coli* ribosome upon telithromycin binding [7,34]. In *D. radiodurans*, a eubacterium sharing a very high level of homology with *E. coli*, as well as with many pathogens, the aryl/alkyl extensions of both telithromycin [13,33] and RU69874 are located in a distance permitting van der Waals interactions with this nucleotide. As mentioned above, the flexible domain II nucleotide U790 provides another prominent interaction with the macrolides erythromycylamine and RU69874. In D50S, nucleotide U790 sticks into the interior of the tunnel, and the structure of its D50S complex with RU69874, as well as with the ketolides cethromycin [11] and telithromycin [13,33], determined by three independent crystallographic studies, indicate that its conformation varies among the native D50S and its complexes (Figs. 5B, D), thus supporting drug-dependent motion of U790. In 77.89 % of all bacteria, nucleotide 790 is a uridine, including *E. coli* and *H. marismortui* [43]. However, all *Streptococci* bacteria carry adenine in this position, and this difference can account for the remarkable low MIC values for telithromycin in *Streptococci*, compared to other bacterial strains as well as to other macrolides [20,38,44–46]. It could also offer an explanation for the marginal effect of the A→G mutation in position 2058 on the susceptibility of telithromycin to *Streptococci,* while conferring resistance to the drug in *Mycobacteria*, which carries U in position 790 [43]. On the other hand, telithromycin and RU69874 binding conformations to *Streptococci* ribosomes may be more similar to those observed in the D50S complexes, providing some conformational rearrangement of the base in position 790, regardless of its identity, adenosine.

Compared to its location in D50S, in unbound *E. coli* [47] as well as in *H. marismortui*, U790 faces the opposite direction and is buried in the tunnel wall. Therefore, it may not be available for interactions with macrolides unless undergoing major drug-dependent conformational rearrangements (Fig. 5D). The structure of mH50S in complex with telithromycin [26] indicates that this motion did not occur. Indeed, in mH50S the aryl/alkyl arm of telithromycin does not reach domain II. Instead, it bends toward the opposite direction, partially overlapping the common position of the cladinose, and stacks on U2609 (Fig. 5C), which in mH50S is shifted toward the interior of the macrolide binding pocket by ~3.5 Å with respect to the position of its counterparts in D50S (Fig. 5C). Hence, it appears that a difference of ~3.5 Å in the position of a single component of the binding pocket may prevent the stretching of the drug across the tunnel, thus leading to a striking difference in the drug's effectiveness.

CONCLUSIONS

Macrolides belong to an antibiotic family possessing common chemical elements with small differences introduced synthetically. As for previously investigated structures, the new crystal structures of complexes of *D. radiodurans* large ribosomal subunit with various macrolides of 14-, 15-, and 16-membered macrolactone ring demonstrate that although all macrolides bind in a specific pocket at the ribosomal exit tunnel, their interactions with the ribosome may be different, indicating that chemical properties can govern the antibiotic binding modes. Analysis of the structures of these complexes elucidated the explicit binding contributions of each of the structural elements of the individual antibiotics and showed that 23S RNA nucleotides involved in macrolide binding may undergo conformational rearrangements for maximizing binding interactions. The variability in the conformations of macrolide binding pockets among the different bacterial species seems to give rise to the drug's altered level of effectiveness. Consequently, it provides crucial information for structure-based drug design.

METHODS

Base and amino acid numbering: We used *E. coli* nucleotide numbers throughout. In specific cases, the number includes the name of the bacterial source (i.e., [ACGU]####Dr, and [ACGU]####Hm are numbered according to the sequence of 23S RNA from *D. radiodurans* and *H. marismortui*, respectively). 23S rRNA sequence alignments were based on the 2D structure diagrams obtained from [43].

Obtaining antibiotics-complex crystals: Crystals of D50S ribosomal subunit were obtained as previously described [8]. Co-crystallization was carried out in the presence of seven-fold excesses of RU69874. Soaking was performed for erythromycylamine and josamycin in solutions containing 0.01 mM of the respective antibiotic.

X-ray diffraction: Data were collected at 85 K from shock-frozen crystals with synchrotron radiation beam. Data were recorded on ADSC-Quantum 4 or APS-CCD detectors, and processed with HKL2000 [48] and the CCP4 suite [49]. See Table 1 for data statistics.

Localization and refinement: The native structure of D50S was refined against the structure factor amplitudes of the antibiotic complex, using rigid body refinement as implemented in CNS [50]. For free R-factor calculation, 5 % of the data were omitted during refinement. The antibiotic site was readily determined from sigmaA weighted difference maps. The quality of the difference maps revealed unambiguously the position and orientation of each of the three macrolides, and further refinement was carried out using CNS.

Coordinates and figures: 3D figures were produced with PyMOL [51], using the Protein Data Bank coordinates. The ribosome–antibiotic interactions were originally determined with LigPlot [52]. Final coordinates have been deposited in the Protein Data Bank under accession numbers 2O43, 2O44, and 2O45.

ACKNOWLEDGMENTS

We thank Frank Schluenzen and Joerg Harms as well as all members of the ribosome groups of the Weizmann Institute, of MPG for Ribosome Structure, Hamburg, and of MPI for Molecular Genetics, Berlin. X-ray diffraction data were collected at ID19, Argonne Photon Source/Argonne National Laboratory (APS/ANL) as well as ID14-4 and ID29, European Synchrotron Radiation Facility/European Molecular Biology Laboratory (ESRF/EMBL). Support was provided by U.S. National Institutes of Health (GM34360), and the Kimmelman Center for Macromolecular Assemblies. AY holds the Helen and Martin Kimmel Professorial Chair.

REFERENCS

1. E. Cundliffe. *Antibiotic Inhibitors of Ribosome Function*, John Wiley, London (1981).
2. M. Gaynor, A. S. Mankin. *Curr. Top. Med. Chem.* **3**, 949 (2003).
3. T. Auerbach, A. Bashan, A. Yonath. *Trends Biotechnol.* **22**, 570 (2004).
4. A. Yonath, A. Bashan. *Annu. Rev. Microbiol.* **58**, 233 (2004).
5. T. Hermann. *Curr. Opin. Struct. Biol.* **23**, 23 (2005).
6. J. Poehlsgaard, S. Douthwaite. *Nat. Rev. Microbiol.* **3**, 870 (2005).
7. S. Douthwaite, L. H. Hansen, P. Mauvais. *Mol. Microbiol.* **36**, 183 (2000).
8. J. Harms, F. Schluenzen, R. Zarivach, A. Bashan, S. Gat, I. Agmon, H. Bartels, F. Franceschi, A. Yonath. *Cell* **107**, 679 (2001).
9. F. Schluenzen, R. Zarivach, J. Harms, A. Bashan, A. Tocilj, R. Albrecht, A. Yonath, F. Franceschi. *Nature* **413**, 814 (2001).
10. J. Harms, H. Bartels, F. Schlunzen, A. Yonath. *J. Cell Sci.* **116**, 1391 (2003).
11. F. Schluenzen, J. M. Harms, F. Franceschi, H. A. Hansen, H. Bartels, R. Zarivach, A. Yonath. *Structure* **11**, 329 (2003).
12. R. Berisio, F. Schluenzen, J. Harms, A. Bashan, T. Auerbach, D. Baram, A. Yonath. *Nat. Struct. Biol.* **10**, 366 (2003).
13. R. Berisio, J. Harms, F. Schluenzen, R. Zarivach, H. A. Hansen, P. Fucini, A. Yonath. *J. Bacteriol.* **185**, 4276 (2003).
14. J. Harms, F. Schlünzen, P. Fucini, H. Bartels, A. Yonath. *BMC Biol.* **2**, 4;1 (2004).
15. F. Schluenzen, E. Pyetan, P. Fucini, A. Yonath, J. Harms. *Mol. Microbiol.* **54**, 1287 (2004).
16. L. Katz, G. W. Ashley. *Chem. Rev.* **105**, 499 (2005).
17. W. S. Champney, C. L. Tober, R. Burdine. *Curr. Microbiol.* **37**, 412 (1998).
18. W. S. Champney, C. L. Tober. *Curr. Microbiol.* **42**, 203 (2001).
19. W. S. Champney, N. Mentens, K. Zurawick. *Curr. Microbiol.* **49**, 239 (2004).
20. K. Falzari, Z. Zhu, D. Pan, H. Liu, P. Hongmanee, S. G. Franzblau. *Antimicrob. Agents Chemother.* **49**, 1447 (2005).
21. L. Xiong, Y. Korkhin, A. S. Mankin. *Antimicrob. Agents Chemother.* **49**, 281 (2005).
22. C. J. Lai, B. Weisblum. *Proc. Natl. Acad. Sci. USA* **68**, 856 (1971).
23. E. C. Boettger, B. Springer, T. Prammananan, Y. Kidan, P. Sander. *EMBO Rep*. **2,** 318 (2001).
24. A. S. Mankin. *Mol. Biol. (Moscow)* **35**, 509 (2001).
25. B. Vester, S. Douthwaite. *Antimicrob. Agents Chemother.* **45**, 1 (2001).
26. D. Tu, G. Blaha, P. B. Moore, T. A. Steitz. *Cell* **121**, 257 (2005).
27. J. L. Hansen, J. A. Ippolito, N. Ban, P. Nissen, P. B. Moore, T. A. Steitz. *Mol. Cells* **10**, 117 (2002).
28. D. J. Hardy, D. M. Hensey, J. M. Beyer, C. Vojtko, E. J. McDonald, P. B. Fernandes. *Antimicrob. Agents Chemother.* **32**, 1710 (1988).
29. G. G. Zhanel, M. Walters, A. Noreddin, L. M. Vercaigne, A. Wierzbowski, J. M. Embil, A. S. Gin, S. Douthwaite, D. J. Hoban. *Drugs* **62**, 1771 (2002).

30. H. A. Kirst, L. C. Creemer, J. W. Paschal, D. A. Preston, W. E. Alborn Jr., F. T. Counter, J. G. Amos, R. L. Clemens, K. A. Sullivan, J. M. Greene. *Antimicrob. Agents Chemother.* **39**, 1436 (1995).
31. G. Garza-Ramos, L. Xiong, P. Zhong, A. Mankin. *J. Bacteriol.* **183**, 6898 (2001).
32. K. Nitta, K. Yano, F. Miyamoto, Y. Hasegawa, T. Sato. *J. Antibiot. (Tokyo)* **20**, 181 (1967).
33. D. N. Wilson, J. M. Harms, K. H. Nierhaus, F. Schlunzen, P. Fucini. *Biol. Chem.* **386**, 1239 (2005).
34. L. H. Hansen, P. Mauvais, S. Douthwaite. *Mol. Microbiol.* **31**, 623 (1999).
35. S. M. Poulsen, C. Kofoed, B. Vester. *J. Mol. Biol.* **304**, 471 (2000).
36. M. Lovmar, T. Tenson, M. Ehrenberg. *J. Biol. Chem.* **279**, 53506 (2004).
37. H. A. Kirst, J. E. Toth, M. Debono, K. E. Willard, B. A. Truedell, J. L. Ott, F. T. Counter, A. M. Felty-Duckworth, R. S. Pekarek. *J. Med. Chem.* **31**, 1631 (1988).
38. F. Depardieu, P. Courvalin. *Antimicrob. Agents Chemother.* **45**, 319 (2001).
39. S. Pereyre, C. Guyot, H. Renaudin, A. Charron, C. Bebear, C. M. Bebear. *Antimicrob. Agents Chemother.* **48**, 460 (2004).
40. P. M. Furneri, G. Rappazzo, M. P. Musumarra, P. Di Pietro, L. S. Catania, L. S. Roccasalva. *Antimicrob. Agents Chemother.* **45**, 2958 (2001).
41. P. Pfister, N. Corti, S. Hobbie, C. Bruell, R. Zarivach, A. Yonath, E. C. Bottger. *Proc. Natl. Acad. Sci. USA* **102**, 5180 (2005).
42. A. Yonath. *Annu. Rev. Biochem.* **74**, 649 (2005).
43. J. J. Cannone, S. Subramanian, M. N. Schnare, J. R. Collett, L. M. D'Souza, Y. Du, B. Feng, N. Lin, L. V. Madabusi, K. M. Iler, N. Pande, Z. Shang, N. Yu, R. R. Gutell. *BMC Bioinformatics* **3**, 1 (2002).
44. N. Rastogi, K. S. Goh, M. Berchel, A. Bryskier. *Antimicrob. Agents Chemother.* **44**, 2848 (2000).
45. A. Tait-Kamradt, T. Davies, M. Cronan, M. R. Jacobs, P. C. Appelbaum, J. Sutcliffe. *Antimicrob. Agents Chemother.* **44**, 2118 (2000).
46. P. Pfister, S. Jenni, J. Poehlsgaard, A. Thomas, S. Douthwaite, N. Ban, E. C. Boettger. *J. Mol. Biol.* **342**, 1569 (2004).
47. B. S. Schuwirth, M. A. Borovinskaya, C. W. Hau, W. Zhang, A. Vila-Sanjurjo, J. M. Holton, J. H. D. Cate. *Science* **310**, 827 (2005).
48. Z. Otwinowski, W. Minor. In *Methods in Enzymology, Macromolecular Crystallography, Part A*, Vol. 276, C. W. Carter Jr., R. M. Sweet (Eds.), p. 307, Academic Press, London (1997).
49. S. Bailey. *Acta Crystallogr., Sect. D* **50**, 760 (1994).
50. A. T. Brunger, P. D. Adams, G. M. Clore, W. L. DeLano, P. Gros, R. W. Grosse-Kunstleve, J. S. Jiang, J. Kuszewski, M. Nilges, N. S. Pannu, R. J. Read, L. M. Rice, T. Simonson, G. L. Warren. *Acta Crystallogr., Sect. D* **54**, 905 (1998).
51. W. L. DeLano. Scientific LLC (<http://pymol.sourceforge.net/>) San Carlos, CA, USA (2002).
52. A. C. Wallace, R. A. Laskowski, J. M. Thornton. *Protein Eng.* **8**, 127 (1995).
53. A. Bashan, I. Agmon, R. Zarivach, F. Schluenzen, J. Harms, R. Berisio, H. Bartels, F. Franceschi, T. Auerbach, H. A. S. Hansen, E. Kossoy, M. Kessler, A. Yonath. *Mol. Cells* **11**, 91 (2003).